# Experimental study on R487A as an alternative refrigerant for household heat pump air conditioners

Jialiang Hua[a], Guogeng He[a,*], Jun Xiong[b], Aihua Wu[a], Zhihao Zhang[a], Xingming Wang[a]

[a] School of Energy and Power Engineering, Huazhong University of Science and Technology, Wuhan 430074, China
[b] TCL Air Conditioner (Zhongshan) Co., Ltd., Guangdong 528400, China

**Abstract**

Household air conditioners with heat pump functionality are becoming increasingly popular in the consumer market. However, high global warming potential (GWP) refrigerants remain the primary working fluid in air conditioning, raising environmental concerns. To promote low-carbon development, a hydrocarbon mixture refrigerant, R487A—composed of ethane (R170) and propylene (R1270)—was investigated as an environmentally friendly alternative to R32 in this paper. R487A possesses favorable thermophysical properties, including higher latent heat, and lower operating pressure. Experimental study was conducted on a household heat pump air conditioner to compare the cycle performance of R32 and R487A under same conditions. Results show that with a 12 $cm^3$/rev compressor, R487A can achieves the same cooling and heating capacities as R32 with comparable COP, while significantly reducing discharge temperature and system pressure. With optimized compressor and appropriate heat exchanger configuration, the system performance of R487A can closely match R32. Owing to its low GWP, reduced charge, and compatibility with existing designs, R487A offers a promising and practical transitional solution for developing countries pursuing low-cost, low-GWP refrigerants and contributing to global carbon emission reduction.



*Keywords: Hydrocarbon refrigerant; Zeotropic misture; Heat pump air conditioner; Carbon emission reduction; Experimental study;*

## 1. Introduction

China is not only the world's largest producer of household air conditioners but also one of the leading countries in terms of consumer demand, particularly for units capable of both cooling and heating [1]. This dominant position largely stems from the climatic characteristics of its densely populated regions, which are subject to both hot summers and cold winters, while centralized heating systems remain limited in coverage. Consequently, modern household air conditioners in China predominantly adopt heat pump technology for space heating, which provides substantially higher energy efficiency than conventional electric resistance heaters.

In terms of refrigerant usage, R32 and R410A—two widely used hydrofluorocarbons (HFCs)—have long dominated the household air conditioner market. Since China's ratification of the Kigali Amendment to the Montreal Protocol in 2021 [2], the country has been accelerating the phase-out of hydrochlorofluorocarbons (HCFCs) with Ozone Depletion Potential (ODP) and the gradual reduction of HFCs with high Global Warming Potential (GWP). The GWP values of R410A and R32 are 2100 and 771 [3], respectively, classifying them as high-GWP refrigerants that are explicitly targeted for phase-down measures. According to analyses reported by the World Meteorological Organization (WMO) and the United Nations Environment Programme (UNEP), China is expected to remain a leading emitter of R32 in the coming decades [4]. Consequently, both R32 and R410A can only serve as transitional refrigerants. The identification and deployment of low-GWP alternatives have become a critical and urgent challenge for China, given its leading role as the world's largest producer and consumer of refrigeration and air conditioner equipment.

In recent years, light-mass natural hydrocarbons (HCs) have attracted increasing attention due to their zero ODP and extremely low GWP, as well as their excellent thermodynamic properties. Typical representatives

* Corresponding author. *E-mail address:* gghe@mail.hust.edu.cn

include propane (R290), isobutane (R600a), and propylene (R1270), etc. Among them, R600a has already been widely adopted in household refrigerators and freezers [5, 6]. Chang et al. [7] conducted an experimental comparison of the cycle performance of R290, R1270, R600a and R600 in a heat pump system and found that the R1270 system had the best performance, achieving slightly higher energy efficiency and heating capacity than the R22 system. Longo et al. [8] studied the evaporation characteristics of R1270 and compared them with the characteristics of R404A in a smooth tube, finding that R1270 had a lower frictional pressure drop. While R290 has recently gained significant research and industrial interest for applications in air conditioners and heat pump systems [9-11]. Owing to its favorable thermophysical properties and energy efficiency, R290 is regarded as a promising candidate for replacing R32.

However, the volumetric capacity of R290 is only about half of R32. Consequently, direct substitution would require substantial redesign of the existing R32 compressors, including an increase in displacement volume, which would considerably raise system modification and manufacturing costs. As such, employing R290 as a direct replacement for R32 is not considered an economically viable option, particularly for developing countries.

To address this issue, the present study proposes a mixed refrigerant R487A composed of ethane (R170) and propylene (R1270) as an alternative working fluid for R32 in household heat pump air conditioners. The proposed mixture can achieve cooling and heating capacities as well as energy efficiency comparable to those of R32, while maintaining compatibility with the original system configurations. This approach offers a cost-effective pathway for system retrofitting and has strong potential for large-scale deployment in developing countries. The gradual replacement of HFCs with such HCs can facilitate the fulfillment of the Kigali Amendment obligations and accelerate the transition toward low-GWP refrigeration technologies.

## 2. Theoretical analysis

R487A is a mixed refrigerant of ethane (R170) and propylene (R1270) with an ODP of 0 and a $GWP_{100}$ of less than 2 [3]. As a replacement for R32, R487A can rapidly reduce $CO_2$-equivalent emissions in developing countries. Its basic thermophysical properties are listed in Table 1obtained from the REFPROP 10.0 [12]. Being a light-mass hydrocarbon refrigerant, R487A has a higher latent heat than R32, which results in a higher cooling capacity per unit mass and thus requires a smaller refrigerant charge. Also, R487A has a density approximately half that of R32, meaning that the actual charge in a system of the same size should be roughly 60% of that used for R32. However, it is important to note that hydrocarbons are highly flammable. According to ASHRAE Standard [13], R487A is classified as safety group A3. Therefore, during testing and application, strict control over the system charge, enhanced leak detection, and leak prevention measures are essential to ensure safety. In this study, experiments were conducted in an explosion-proof enthalpy difference laboratory equipped with gas detector and emergency venting facilities.

In terms of transport and thermophysical performance, R487A exhibits a thermal conductivity comparable to R32, and a lower viscosity, which reduces flow resistance. Its higher specific heat often leads to a lower adiabatic index and lower discharge temperature. Additionally, R487A features a lower standard boiling point and a higher critical temperature, providing a wider operational range that can accommodate both high-temperature cooling and low-temperature heating requirements. One of the most distinctive thermodynamic characteristics of R487A is its temperature glide of approximately 15 K at atmospheric pressure. In principle, a large temperature glide can improve heat transfer effectiveness by enhancing temperature matching between the refrigerant and the secondary fluid. However, it also increases the complexity of heat exchanger design and system control. A mismatch between the refrigerant phase-change temperature profile and the secondary fluid temperature profile may result in local pinch points and incomplete utilization of the heat transfer surface. In addition, local composition variations during phase change, as well as maldistribution of refrigerant within the heat exchanger, may alter thermophysical properties and reduce system efficiency, which is particularly critical for high-glide mixtures. It should be noted that the operating pressure of refrigeration systems is typically much higher than atmospheric pressure. With increasing pressure, the volatility difference among the components decreases, leading to a reduction in temperature glide. For R487A, the temperature glide decreases to approximately 7–11 K under typical household air conditioner operating conditions. Meanwhile, the air-side temperature variation in heat exchanger is typically 5–8 °C under test conditions and can be even larger under practical operating conditions. Therefore, refrigerants with relatively large temperature, can theoretically be well adapted to air-conditioning applications.

The theoretical cycle calculations were performed using the cooling and heating operating conditions listed in Tables 2 and 3. For the zeotropic refrigerant R487A, the evaporating pressure was taken as the mean of the bubble point and dew point pressures at 7.2 °C, while the condensing pressure was taken as the mean of the bubble point and dew point pressures at 54.4 °C; the same method was applied for the heating conditions. The volumetric efficiency of the compressor was assumed to be 0.9, and the isentropic efficiency 0.8. The results indicate that the volumetric capacity of R487A is approximately 85% of that of R32. When using a compressor with the same displacement as R32 (9.8 cm³/rev), the compressor frequency must be increased to achieve the same capacity. However, this may cause the compressor to operate away from its factory-set optimal frequency. Using a larger displacement such as R32 compressor (12 cm³/rev) can overcome this limitation. The cycle performance, in terms of coefficient of performance (COP), is essentially comparable to R32. Furthermore, R487A exhibits lower discharge temperatures and condensing pressures than R32, which is beneficial for enhancing overall compressor durability under high-temperature cooling and high-load heating conditions.

Plotting the data points on a *T–s* diagram allows for a more intuitive visualization of the cycle characteristics. As shown in Figure 1, the saturated liquid line of R32 is steeper than that of R487A, meaning that a relatively small amount of heat exchange can achieve substantial subcooling. This indicates that, for R32, enhancing subcooling is an efficient optimization strategy. In contrast, R487A, being a zeotropic refrigerant, undergoes a continuous temperature drop during condensation. Its system efficiency is improved by optimizing temperature matching rather than relying on a large subcooling that would be necessary for a single-component refrigerant. Due to R32's relatively gentle saturated vapor line and higher adiabatic index, the superheat must be strictly controlled to prevent excessive discharge temperatures. On the other hand, R487A's steeper saturated vapor line and lower adiabatic index make its discharge temperature less sensitive to variations in superheat. However, it is important to note that R487A, as a hydrocarbon refrigerant, exhibits a large two-phase region during heating. While this provides high capacity for heat transfer, it may naturally result in a low evaporator outlet superheat. To mitigate this, the heat exchanger must have a sufficiently large heat transfer area.

Table 1. Thermodynamic properties of refrigerants [3][12][13].

| Properties | R32 | R487A |
|---|---|---|
| Molar mass | 52.02 | 38.97 |
| Latent heat (kJ/kg) | 382.14 | 477.46 |
| Liquid thermal conductivity (W/m.K) | 0.18 | 0.15 |
| Vapor thermal conductivity (W/m.K) | 0.0086 | 0.010 |
| Liquid specific heat capacity (kJ/kg.K) | 1.59 | 2.19 |
| Vapor specific heat capacity (kJ/kg.K) | 0.87 | 1.35 |
| Liquid viscosity x$10^{-4}$ (Pa·s) | 2.78 | 2.11 |
| Vapor viscosity x$10^{-4}$ (Pa·s) | 0.092 | 0.062 |
| Normal boiling point (°C) | -51.65 | -68.76 |
| Temperature glide (K) | - | 15.32 |
| Critical pressure (kPa) | 5782 | 5039 |
| Critical temperature (°C) | 78.11 | 80.18 |
| Critical density (kg/m$^3$) | 424.0 | 223.38 |
| Safety group | A2L | A3 |
| ODP | 0 | 0 |
| $GWP_{100}$ | 771 | <2 |

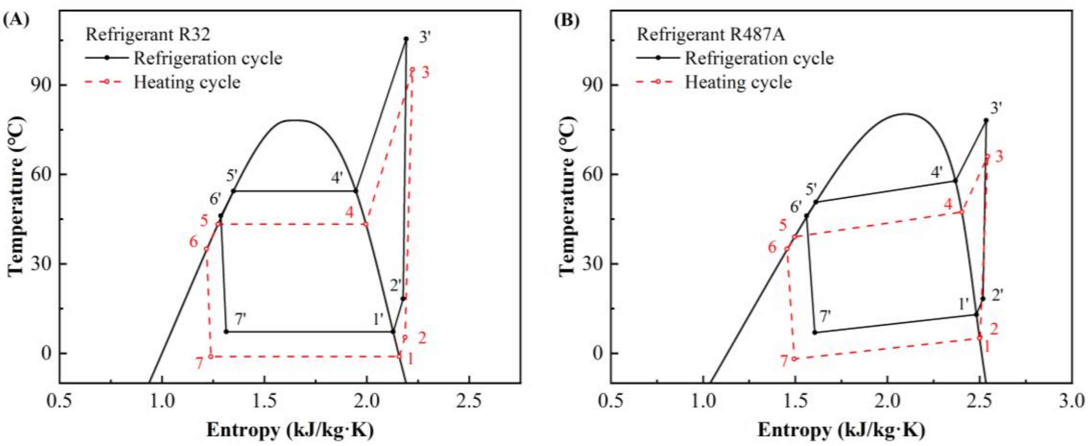


Figure 1. Theoretical cycle *T-s* diagram for cooling and heating of R32 and R487A.

Table 2. Theoretical refrigeration cycle calculation.
(Evaporation temperature 7.2℃; suction temperature 18.3℃; condensation temperature 54.4℃; condenser outlet temperature 46.1℃)

| Refrigerant (Compressor displacement) | Compressor frequency (Hz) | Rotational speed (rpm) | Refrigerant flow rate (kg/s) | Evaporation Pressure (MPa) | Condensation Pressure (MPa) | Suction specific volume ($m^3$/kg) | Volumetric cooling capacity (kJ/$m^3$) | Discharge temperature (℃) | Cooling capacity (kW) | COP |
|---|---|---|---|---|---|---|---|---|---|---|
| R32 （9.8cm³/rev） | 50 | 3020 | 0.0114 | 1.02 | 3.47 | 0.039 | 6236.13 | 111.11 | 2.77 | 3.26 |
| R487A （9.8cm³/rev） | 59 | 3563 | 0.0108 | 1.07 | 3.10 | 0.049 | 5320.41 | 81.26 | 2.79 | 3.31 |
| R487A （12cm³/rev） | 50 | 3020 | 0.0112 | 1.07 | 3.10 | 0.049 | 5320.41 | 81.26 | 2.89 | 3.31 |

Table 3. Theoretical heat pump cycle calculation.
(Evaporation temperature -1.1℃; suction temperature 5.4℃; condensation temperature 43.3℃; condenser outlet temperature 35℃)

| Refrigerant (Compressor displacement) | Compressor frequency (Hz) | Rotational speed (rpm) | Refrigerant flow rate (kg/s) | Evaporation Pressure (MPa) | Condensation Pressure (MPa) | Suction specific volume ($m^3$/kg) | Volumetric heating capacity (kJ/$m^3$) | Discharge temperature (℃) | Heating capacity (kW) | COP |
|---|---|---|---|---|---|---|---|---|---|---|
| R32 （9.8cm³/rev） | 85 | 5133 | 0.0155 | 0.78 | 2.68 | 0.049 | 6605.64 | 95.20 | 5.00 | 4.45 |
| R487A （9.8cm³/rev） | 96 | 5797 | 0.0145 | 0.86 | 2.48 | 0.059 | 5876.46 | 66.04 | 5.00 | 4.53 |
| R487A （12cm³/rev） | 85 | 5133 | 0.0156 | 0.86 | 2.48 | 0.059 | 5876.46 | 66.04 | 5.43 | 4.53 |

## 3. Experimental method

R487A is a zeotropic refrigerant with temperature glide, which allows the utilization of its temperature variation during phase change to reduce heat transfer losses and improve energy efficiency. However, this feature requires that the heat exchanger be arranged in a counter-flow configuration relative to the air, both in cooling and heating modes; otherwise, not only will the energy-saving effect of the temperature glide be lost, but irreversible heat transfer losses may also increase. In contrast, widely produced and used air conditioners typically employ single-component refrigerants such as R32 or R290, or azeotropic mixtures such as R410A, whose temperatures remain nearly constant during phase change. Therefore, even with a co-flow heat exchanger, performance degradation is relatively small. Based on the temperature glide characteristics of R487A, a single-row 7 mm micro-fin spiral tube heat exchanger was employed for the outdoor unit, as shown in Figure 2(A). This design maintains the heat transfer area while avoiding issues related to counter-flow arrangement. For the indoor unit, as shown in Figure 2(B), a two-row 5 mm micro-fin spiral tube heat exchanger was used. During cooling tests, the inlet and outlet were arranged in a counter-flow configuration relative to the air; for heating tests, the inlet and outlet were swapped while maintaining the counter-flow configuration. The specific parameters of the heat exchangers are listed in Table 4.

In addition to the indoor and outdoor heat exchangers, the system employed compressors designed for R32 with displacements of 9.8 cm³/rev and 12 cm³/rev, using polyol ester (POE) as the lubricant. Using the R32 system with a 9.8 cm³/rev compressor as the control group, R487A was tested with compressors of different displacements, aiming to achieve the same cooling/heating capacity as R32 for performance comparison. The expansion device was a universal electronic expansion valve (EEV) with a 2.2 mm orifice. The dimensions and rotational speeds of both the indoor and outdoor fans were identical for different refrigerant. Experimental tests were conducted in an explosion-proof enthalpy difference laboratory, as shown in Figure 3, equipped with gas detection devices to monitor gas leaks and allow for timely venting. Pressure and temperature sensors were installed at the inlets and outlets of both the heat exchangers and the compressor, while the air parameters at the heat exchanger inlets and outlets were measured through laboratory. The tests included four cooling and heating operating conditions, as listed in Table 5. Prior to testing each condition, the refrigerant charge corresponding to the maximum COP was determined under high-temperature cooling (Cooling-1) for both R32 and R487A and used as the test charge. For R32 with a 9.8 cm³/rev compressor, the charge was 620g. R487A charged with a 9.8 cm³/rev compressor required 360g, approximately 58% of the R32 charge. When R487A was tested with a 12 cm³/rev compressor, the required charge increased to 380g, approximately 61% of that for R32, due to the increased lubricant volume.

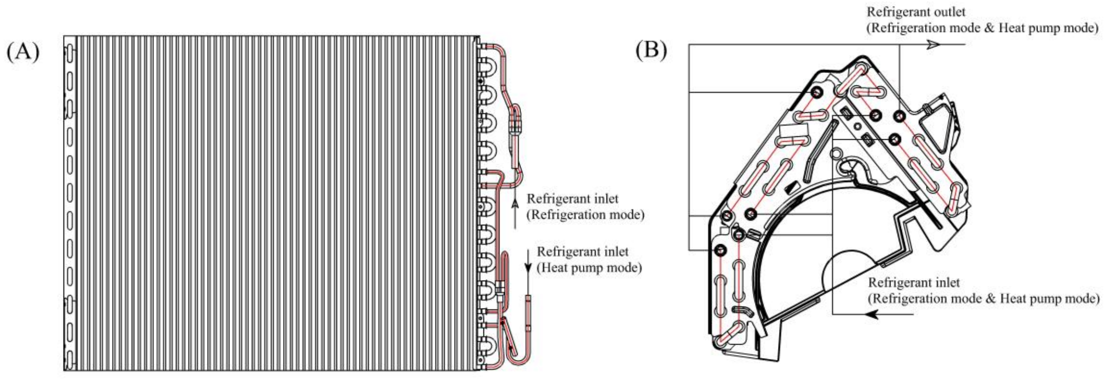


Figure 2. Indoor and outdoor heat exchangers.

Table 4. Heat exchanger parameters.

| Properties | Indoor heat exchanger | Outdoor heat exchanger |
|---|---|---|
| Tube diameter (mm) | 5 | 7 |
| Tube thickness (mm) | 0.37 | 0.32 |
| Tube length (mm) | 637 | 778 |
| Enhance internal structure | Micro-fin spiral tube | Micro-fin spiral tube |
| Internal fin number | 54 | 65 |
| Spiral angle (°) | 16 | 16 |
| Spiral pitch (mm) | 0.2 | 0.2 |
| Tube row number | 2 | 1 |
| Tube number | 32 | 24 |
| Outer fin type | Louver fin | Wavy fin |
| Outer fin thickness (mm) | 0.095 | 0.095 |
| Outer fin spacing (mm) | 1.3 | 1.3 |

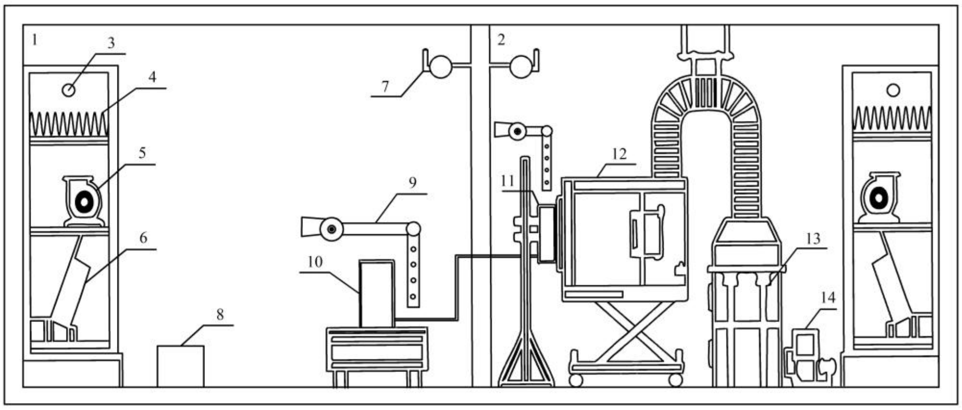


Figure 3. The enthalpy difference laboratory: 1. Outdoor lab; 2. Indoor lab; 3. Humid air inlet; 4. Heater; 5. Circulating fan; 6. Evaporator; 7. Gas detector; 8. Exhaust vent; 9. Air sampler; 10. Outdoor unit; 11. Indoor unit; 12. Air volume measuring apparatus; 13. Air nozzle; 14. Static pressure fan.

Table 5. Test condition parameters.

| Testing conditions (Designation) | Indoor dry bulb temperature (℃) | Indoor wet bulb temperature (℃) | Outdoor dry bulb temperature (℃) | Outdoor wet bulb temperature (℃) |
|---|---|---|---|---|
| High-temperature (Cooling-1) | 27 | 19 | 35 | 24 |
| Low-temperature (Cooling-2) | 27 | 19 | 29 | 19 |
| High-temperature (Heating-1) | 20 | 15 | 7 | 6 |
| Low-temperature (Heating-2) | 20 | 15 | 2 | 1 |

## 4. Results and discussion

The experimental groups consisted of R32 with a 9.8 cm³/rev compressor, R487A with a 9.8 cm³/rev compressor, and R487A with a 12 cm³/rev compressor. The performance of R32 was used as the baseline for evaluating R487A under each testing condition. During the tests, the electronic expansion valve was adjusted to maintain the compressor inlet in a superheated state as much as possible, aiming to identify the optimal energy efficiency point. The indoor unit was always arranged in a counter-flow configuration relative to the air. Figure 4 presents the measured indoor capacities, COP, system power consumption, and pressure ratios for all experimental groups, while Table 6 summarizes detailed test results, including compressor inlet and outlet pressures, heat exchanger outlet subcooling and superheat, and measured capacities.

As shown in Figure 4, to achieve the same capacity as R32, R487A with the same compressor displacement required an increase in compressor frequency of more than 20% to meet the basic mass flow demand. Under low-temperature heating (Heating-2), R487A with the 9.8 cm³/rev compressor could not meet the required capacity, as the compressor frequency was already close to its operational limit. Increasing the frequency of the same-displacement compressor resulted in a noticeable reduction in energy efficiency. Under cooling conditions, the COP of R487A was on average approximately 7.1% lower than that of R32. Under high-temperature heating (Heating-1), increasing the frequency by 20 Hz led to a 6.9% reduction in COP compared with R32, indicating that the compressor was operating away from the optimal frequency for these conditions. Assuming the throttling process is isenthalpic, the mass flow rate and approximate volumetric efficiency under each operating condition were calculated, as listed in Table 6. It was observed that, during heating conditions, the R487A compressor suction was often in a two-phase state, especially for the 9.8 cm³/rev compressor. This resulted in a significant drop in volumetric efficiency to approximately 85% of normal operation, leading not only to reduced energy efficiency but also to lower discharge temperatures. This indicates an imbalance between the flow provided by the compressor and expansion valve and the heat exchanger capacity.

When the 12 cm³/rev compressor was used, R487A could achieve cooling and heating capacities comparable to R32 at near-default compressor frequencies. Under these conditions, the average COP under cooling was approximately 97.3% of R32, and 97.5% under Heating-1. Under Heating-2, the COP of R487A reached 2.56, closely matching R32; notably, the R32 compressor frequency had to be increased to 118 Hz to achieve this performance, while R487A achieved comparable or even higher heating capacity at the default 114 Hz, indicating superior energy efficiency for R487A under this condition. Under Heating-1, R487A with the 12 cm³/rev compressor still exhibited slight two-phase suction, whereas other conditions maintained sufficient superheat. As noted in the theoretical analysis above, with decreasing evaporating pressures, the larger latent heat region of R487A may require an increased heat exchanger surface area to fully release energy.

Furthermore, during tests with the 12 cm³/rev compressor, it was observed that, except for the low-temperature heating condition where R487A outperformed R32 in energy efficiency, the evaporating pressures of R487A under all other operating conditions were lower than those of R32. According to the theoretical cycle calculations presented in Chapter 1, under ideal conditions—assuming no heat transfer temperature differences and perfect matching between the heat exchanger and the refrigerant temperature profiles—the system can achieve its maximum ideal efficiency, which represents the optimal direction for system optimization. Under such ideal conditions, the evaporating and condensing pressures of R487A would be expected to lie between those of R32. This indicates that in the current experimental setup, the evaporating pressure of R487A has not yet reached its optimal level.

Under Heating-2 at maximum mass flow rate, a large portion of the refrigerant enters the evaporator, and most of the evaporator surface is utilized for highly efficient two-phase heat transfer. Only a small segment at the end contributes to superheat generation, meaning that the system bottleneck is often limited by the condenser's capacity or the compressor's operational limits, allowing performance closer to the ideal state. At lower frequency conditions, less refrigerant enters the evaporator. The refrigerant evaporates rapidly within a shorter physical length at the evaporator inlet. To absorb sufficient heat in the less efficient superheated region and achieve the target superheat, the inlet refrigerant mass must be limited. Consequently, in order to maintain adequate heat transfer for superheating, the electronic expansion valve must restrict the flow significantly, which drastically reduces the proportion of the high-efficiency two-phase region and lowers the evaporator heat transfer coefficient. As a result, the system is forced to reduce the evaporating pressure to increase the conventional temperature difference and achieve the target heat transfer capacity, ultimately reducing energy efficiency. This explains why, under cooling conditions, the 12 cm³/rev R487A system still requires an increase of 1–3 Hz in compressor frequency to achieve the same capacity as R32. In this case, the evaporator represents the primary system bottleneck.

In addition, previous studies on boiling heat transfer in micro-fin spiral tubes have shown that mass flux and heat flux significantly affect the boiling heat transfer coefficient of R487A [14]. Under identical mass flux, R487A exhibits a higher boiling heat transfer coefficient than R32. However, in practical systems, for the same heat capacity, the required mass flow rate of R487A is generally lower than that of R32, which partially suppresses its heat transfer enhancement. Furthermore, at the same evaporation temperature, increasing the heat flux by three times can increase the boiling heat transfer coefficient by approximately 70%. Combined with the results of the present study, where the R487A system demonstrates better performance under high-capacity conditions, this observation further highlights the strong dependence of R487A boiling heat transfer performance on heat flux. Future work will prioritize the development of heat exchanger designs specifically tailored for R487A, with particular emphasis on enhancing heat transfer effectiveness under varying conditions and accommodating the temperature glide characteristics.

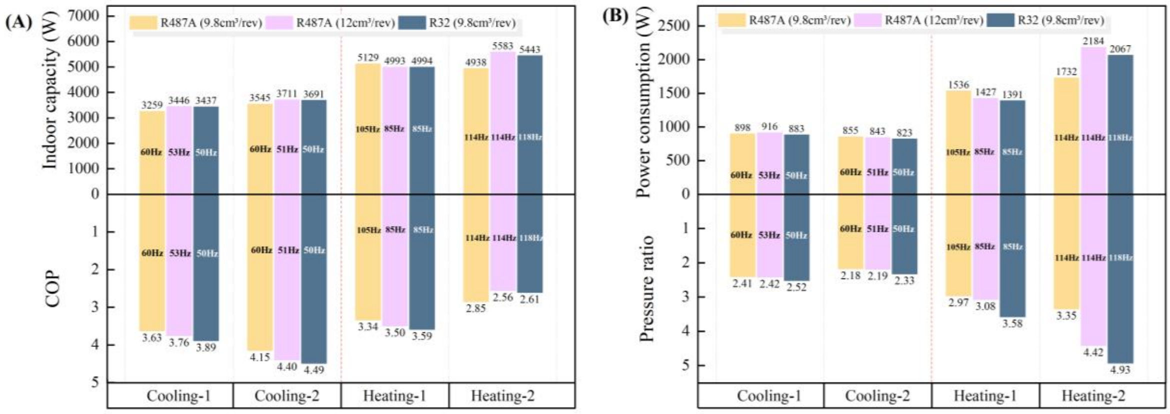


Figure 4. Performance parameters in the test results.

Table 6. Test results summary.

| Refrigerant (Compressor displacement) | Testing conditions | Compressor frequency (Hz) | Suction Pressure (MPa) | Discharge pressure (MPa) | Discharge temperature (°C) | Subcooling degree (°C) | Superheat degree (°C) | Calculated flow rate (kg/s) | Calculated volumetric efficiency | Indoor capacity (W) | COP |
|---|---|---|---|---|---|---|---|---|---|---|---|
| R32 (9.8cm³ /rev) | Cooling-1 | 50 | 1.20 | 3.03 | 77.50 | 10.43 | 2.86 | 0.0137 | 0.87 | 3436.94 | 3.89 |
| | Cooling-2 | 50 | 1.20 | 2.80 | 71.10 | 11.31 | 2.15 | 0.0142 | 0.89 | 3691.32 | 4.49 |
| | Heating-1 | 85 | 0.76 | 2.73 | 82.00 | 18.05 | 0.79 | 0.0154 | 0.89 | 4994.10 | 3.59 |
| | Heating-2 | 118 | 0.60 | 2.96 | 89.10 | 19.81 | 1.25 | 0.0166 | 0.88 | 5443.06 | 2.61 |
| R487A (9.8cm³/rev) | Cooling-1 | 60 | 1.16 | 2.80 | 67.40 | 5.55 | 1.36 | 0.0117 | 0.86 | 3259.19 | 3.63 |
| | Cooling-2 | 60 | 1.17 | 2.55 | 61.00 | 6.71 | 0.53 | 0.0119 | 0.87 | 3545.08 | 4.15 |
| | Heating-1 | 105 | 0.84 | 2.49 | 54.80 | 9.99 | -1.84 | 0.0151 | 0.75 | 5129.09 | 3.34 |
| | Heating-2 | 114 | 0.74 | 2.50 | 55.00 | 10.46 | -3.54 | 0.0146 | 0.72 | 4938.43 | 2.85 |
| R487A (12cm³/rev) | Cooling-1 | 53 | 1.11 | 2.69 | 69.80 | 4.97 | 2.83 | 0.0122 | 0.87 | 3446.28 | 3.76 |
| | Cooling-2 | 51 | 1.19 | 2.61 | 60.50 | 4.12 | 0.69 | 0.0130 | 0.89 | 3711.23 | 4.4 |
| | Heating-1 | 85 | 0.77 | 2.37 | 57.40 | 6.72 | -0.25 | 0.0146 | 0.83 | 4993.00 | 3.5 |
| | Heating-2 | 114 | 0.62 | 2.74 | 75.10 | 13.45 | 0.92 | 0.0149 | 0.88 | 5583.10 | 2.56 |

## 5. Conclusion

An experimental study was conducted to evaluate the thermodynamic performance and practical applicability of the zeotropic hydrocarbon refrigerant R487A in comparison with the refrigerant R32. Experimental results demonstrated that, with the same 9.8 cm³/rev compressor displacement, R487A required 20% higher compressor frequency to match the cooling and heating capacities of R32, leading to a 6–7% reduction in energy efficiency due to operation away from the compressor's optimal frequency. Using a larger 12 cm³/rev compressor effectively restored the system balance, achieving average 97.4% of R32's COP under the same cooling and heating capacity. Under low-temperature heating conditions, R487A even exhibited superior performance, achieving equal or higher heating capacity at a slightly lower compressor frequency.

Further analysis indicated that R487A's evaporating pressure remained below its theoretical optimum under most conditions. At low compressor speeds, insufficient liquid refrigerant entering the evaporator reduced the proportion of two-phase heat transfer and forced a drop in evaporating pressure to maintain the target superheat, lowering system efficiency. Conversely, under high-flow heating, the evaporator operated predominantly in the two-phase region, with the main limitation shifting to the condenser or compressor capacity.

For the safe application of A3 hydrocarbon refrigerants, several mature and proven design strategies can be adopted. Electrical components are sealed and explosion-protected to minimize ignition risks under refrigerant leakage; specifically, a fully sealed electrical control box with sealing gaskets, rubber sealing rings, sealed cable feedthroughs, and a fire-resistant metal enclosure should be employed. In addition, automatic shut-off valves are installed in the refrigerant lines between the outdoor and indoor units to promptly isolate the refrigerant circuit during shutdown or abnormal operation. This prevents excessive refrigerant migration into the indoor unit and reduces the maximum refrigerant release in the event of leakage. Furthermore, minimum safe installation volumes are defined based on the flammability limits of hydrocarbon refrigerants, with appropriate safety margins applied. Future work will explore enhanced outdoor heat exchangers with small tube diameters to further reduce the total refrigerant charge.

Overall, R487A demonstrates promising potential as an eco-friendly zeotropic alternative to R32, offering comparable capacity and cycle efficiency, lower discharge temperature, and better compressor durability. To fully realize its performance advantages, optimization of the evaporator design and precise flow control strategies are essential, ensuring effective utilization of its temperature glide characteristics and stable operation under both cooling and heating conditions.

## Acknowledgements

This work is supported by the TCL Air Conditioner (Zhongshan) Co., Ltd., Guangdong, China.

## References


[1] International Energy Agency (IEA). *The future of cooling in China*. Paris: IEA Publications; 2019.

[2] United Nations Environment Programme (UNEP). *Kigali Amendment to the Montreal Protocol*. Nairobi: UNEP; 2018.

[3] IPCC. *Climate Change 2021 – The Physical Science Basis: Working Group I Contribution to the Sixth Assessment Report of the Intergovernmental Panel on Climate Change*. Cambridge: Cambridge University Press; 2023.

[4] World Meteorological Organization (WMO) / United Nations Environment Programme (UNEP). *Scientific Assessment of Ozone Depletion: 2022*. Geneva: WMO; 2022.

[5] Koh JH, Zakaria Z. *Hydrocarbons as Refrigerants—A Review*. ASEAN Journal of Science and Technology for Development, 2017, 34(1): 35–50.

[6] Wongwises S, Chimres N. *Experimental study of hydrocarbon mixtures to replace HFC-134a in a domestic refrigerator*. Energy Conversion and Management, 2005;46(1):85-100.

[7] Chang YS, Kim MS, Ro ST. *Performance and Heat Transfer Characteristics of Hydrocarbon Refrigerants in a Heat Pump System*. International Journal of Refrigeration, 2000, 23(3): 232–242.

[8] Longo GA, Mancin S, Righetti G, Zilio C. *Hydrocarbon Refrigerants HC290 (Propane) and HC1270 (Propylene) as Low-GWP Long-Term Substitutes for HFC404A: A Comparative Analysis in Vaporization Inside a Small-Diameter Horizontal Smooth Tube*. Applied Thermal Engineering, 2017, 113: 1140–1151.

[9] Harby K. *Hydrocarbons and their mixtures as alternatives to environmentally unfriendly halogenated refrigerants: An updated overview*. Renewable and Sustainable Energy Reviews 2017;73:1247–64.

[10] Ozsipahi M, Kose HA, Kerpicci H, et al. *Experimental study of R290/R600a mixtures in vapor compression refrigeration system*. International Journal of Refrigeration 2022;133:247–58.

[11] Bengtsson P, Eikevik T. *Reducing the global warming impact of a household heat pump dishwasher using hydrocarbon refrigerants*. Applied Thermal Engineering 2016;99:1295–1302.

[12] Lemmon EW, Huber ML, Mclinden MO. *NIST Standard Reference Database 23: REFPROP, Version 10.0*. Gaithersburg: National Institute of Standards and Technology (NIST), 2023.

[13] ASHRAE. *ASHRAE Standard 34-2023: Designation and Safety Classification of Refrigerants*. Atlanta: American Society of Heating, Refrigerating and Air-Conditioning Engineers (ASHRAE), 2023.

[14] Zhang Z, Chen T, Shi L, et al. *Flow boiling heat transfer characteristics of the new hydrocarbon blend R487A in a horizontal tube: an experimental study*. Applied Thermal Engineering 2025: 128097.